STUDIES OF INTENSITY MODULATED LIGHT IN TURBID MEDIA

Diploma paper
by
Claes af Klinteberg

Lund Reports on Atomic Physics, LRAP-139
Lund, June 1993

1 ABSTRACT

This paper describes experiments with a phase-shift technique to enhance the contrast in optical transillumination of turbid media. This technique has applications in light scanning of female breast in order to detect breast cancer.

Usually, phase-resolved methods are based on the cross-correlation technique. Then both the light source and the gain of the detector are modulated with a radio frequency, but with a little difference in the frequencies. The interesting parameters are then measured on the low frequency cross-correlation signal.

In this paper another method is described. Only the light source, a diode laser, is modulated. The AC component of the detected signal is then mixed with the same signal that is used for the modulation. Thus, a DC component proportional to the cosine of the phase lag between the signals is obtained. Differences in the scattering coefficient and the absorption coefficient might be detected by measuring the phase lag and the demodulation of the detected signal.

Preliminary results suggest that the technique might be useful.

CONTENTS

1 Abstract 3

2 Introduction 7
- 2.1 Cancer 7
- 2.2 The Breast 8
- 2.3 Treatment 8
- 2.4 Mammography 8
- 2.5 Ultrasonography 9
- 2.6 Thermography 9
- 2.7 Tomographic Methods 10
- 2.8 Methods Using Visible Light 10
  - 2.8.1 Time Resolved Methods 10
  - 2.8.2 Phase Resolved Methods 12
- 2.9 The Purpose of This Project 13

3 The Interaction of Light With Tissue 15
- 3.1 Reflection 15
- 3.2 Absorption 18
- 3.3 Scattering 19
- 3.4 Theoretical Models 19
  - 3.4.1 Linear Transport Theory 20
  - 3.4.2 The Transport Equation 22
  - 3.4.3 The One-Speed Approximation 24
  - 3.4.4 The Diffusion Approximation 24
  - 3.4.5 Isotropic Sinusoidally Modulated Point Source 28

4 Methods and Materials 37
- 4.1 Experimental Arrangement 37
- 4.2 The Detector 38
- 4.3 The Mixer 38
- 4.4 The Sample 39

5 Results 41

6 Discussion and Conclusions 45
- 6.1 Problems 45
- 6.2 The Future 45
- 6.3 Conclusions 46

7 Acknowledgments 49

8 List of References 51

2 INTRODUCTION

Breast cancer is today one of the most common causes of early death among women. One woman out of 17 will suffer from the disease, i.e. 6% of the female population. To succeed in the treatment of cancer the tumour has to be detected as early as possible. Today the most common method used to detect cancer is mammography. Mammography is a technique based on X-rays, i.e. there is a potential risk of causing mutagenicity, since it is a form of ionising radiation. Therefore a method of screening for breast cancer that does not require the use X-rays would be of considerable clinical benefit.

Different methods using visible light to see through the breast have been made. The first attempt was made by Ewing in 1928 [1]. He simply illuminated the breast with a lamp and looked for shadows of tumours on the other side. The heat production from the lamp made this technique uncomfortable to the patients. In 1929 Cutler developed a method of water cooling, more lenient for the patient [2]. The technique was, however, not very successful and did not gain any general interest at that time. With the rapid development in the field of computers, lasers and theory for tissue optics during the last two decades, new methods involving visible light are being developed.

This paper describes a technique involving phase-resolved laser spectroscopy to improve the contrast in visible light transillumination for breast cancer detection. It also includes a review over different techniques to detect cancer and a theoretical part concerning the interaction of light with tissue.

2.1 CANCER

Cancer is the common name for a pathological condition in which unrestrained growth of abnormal cells takes place in one or more organs in the human body. The cell growth gives rise to a tumour. There are two types of tumours, benign and malignant. A benign tumour grows expansively and is clearly defined. If it is not treated, the only harm that it can cause is through pressure on the surrounding tissue, which in vital organs might cause death. A malignant tumour, on the other hand, will cause death, even if it grows in a hand or a foot. The malignant tumour grows between the normal cells. This makes it very hard to remove all parts of the tumour surgically. The malignant cancer cells can be transported with the lymph and the blood and in that way give rise to new tumours, metastases, in other organs.

In Sweden, as in most western countries, breast cancer is the most frequent form of malignancy. The incidence of breast cancer increases with age, but almost one fifth of the women with breast cancer in Sweden are younger than 50 years [3]. Breast cancer is also the most common cause of death among women aged 40 to 54. It is impossible to determine the exact cause of the cancer, but some factors increase the risk of developing the disease, for example genetic factors, early menarche, late menopause, first pregnancy before 16 years or after 35 years and more than three pregnancies [4].

2.2 THE BREAST

The female breast consists of skin, fat, glandular tissue and connective tissue. There is a considerable periodic variation in the structure of the breast due to the female hormone cycle. There are also variations in the structure during pregnancy and after lactation ceases. Finally, the glandular tissue will at menopause gradually be replaced with fat. This means that it is more difficult to find a cancer tumour in a younger woman than it is in an older one using mammography.

A cancer tumour in the breast gives rise to a dense volume, often with increased concentration of blood vessels. This volume grows continuously and the mean volume doubling time of the tumour is approximately 212 days, with large variations [5]. It can thus be calculated that breast cancer needs about four years to grow from a diametre of 2 mm to a diametre of 10 mm.

2.3 TREATMENT

Carcinoma of the breast is, as earlier mentioned, the most frequent malignant tumour in women and causes more deaths in females than any other type of malignant growth. In order to treat breast cancer successfully, it is important that the tumour is detected as early as possible. The 5-year survival rate of breast cancer treated by segmental mastectomy combined with radiation therapy is 90%, if the diameter of the tumour is less than 4 cm when treated. If the tumour is left untreated the average survival rate is 2.5 years. If the tumour is treated before detectable lymph node metastases have developed, the recurrence rate five years after the treatment is 25%. If lymph node metastases have been developed prior to the treatment, the recurrence rate rises to 50 to 70% [4].

2.4 MAMMOGRAPHY

Today mammography is the most common method used to detect breast cancer. The breast is compressed between two flat plates to a thickness of a few centimetres. On one side of the breast a photographic plate is placed and the other side is radiated with X-rays. On the photographic plate the tumour can be seen as an area where the X-rays have been absorbed more than in the surrounding tissue. To increase the probability to detect tumours, three exposures from different angles are often taken.

Mammography has proven to have a high efficiency of detecting breast cancer [3]. However, there are problems in interpreting the photographic plates due to variations of the structure and density of both tumours and healthy tissue. This sometimes makes it hard to find a large tumour in a breast with a lot of glandular tissue while it is possible to find much smaller tumours, down to 3 to 5 mm, in a fattier breast. Another important factor is the size of the breast. The more the breast can be compressed the easier it is to find a tumour. Because of all these problems the interpreter has to develop some kind of intuition when examining the plates. Another problem is that about 40% of all breast cancers are not seen on a mammogram [4].

Since it is important to find the tumours as early as possible, it is desirable to perform mammography on as many women as possible. On the other hand, mammography uses X-rays that are ionising and therefore there is a potential risk to induce cancer. The risk is of course difficult to estimate. One risk analysis indicates that the benefit to risk ratio in mass-screening with mammography for symptomatic women aged 35 to 49 is about 3.4 to 1 (worst case) with even a lower benefit for younger women [5].

In an American study, Swift *et al.* [7] has shown that persons heterozygous for the ataxia-telangiectasia gene, who make up about 1 percent of the U.S. white population, have an excess risk of cancer, particularly breast cancer in women. They may constitute 9 to 18 percent of all persons with breast cancer in the United States. Further, Swift *et al.* has shown that the ataxia-telangiectasia gene is associated with unusual sensitivity to ionising radiation. Tests with cultured cells supported the theory that doses of ionising radiation below 20 mGy might induce breast cancer in heterozygotes. In other populations, doses above 100 to 200 mGy are needed to induce breast cancer. With these results Swift *et al.* recommends that reliable alternatives to diagnostic X-rays should be considered whenever possible and that measures should be taken to minimise incidental radiation to breast tissue as much as possible during all X-ray examinations. In the specific case of mammography, the risk of radiation induced cancer in heterozygotes may exceed the benefits of early detection. During a mammographic exposure, the glandular tissue of the breast receives 0.5 to 7 mGy. Whether this leads to an excess of breast cancer in women heterozygous for the ataxia-telangiectasia gene remains to be determined, but alternatives to mammography should be considered for these women.

2.5 ULTRASONOGRAPHY

Ultrasound can be used as a diagnostic tool to find volumes with an acoustic impedance different than that of the surrounding tissue. Tumours are different than normal breast tissue in this sense. In this method, an ultrasonic wave is sent into the breast by a transducer. The tumour creates an echo due to a change in acoustic impedance. The echo is detected by the transducer and the result can be analysed and displayed on a monitor. In most studies, however, ultrasound has failed to detect clinically occult cancer. There are also problems in differentiating between benign and malignant solid lesions, which might lead to a high rate of false-positive results. Furthermore, diagnosis in fattier breasts is difficult because of differences in the acoustic impedance between the fat and the connective tissue [3].

2.6 THERMOGRAPHY

Thermography is a method that portrays the biological activity of the breast by translating the invisible infrared heat radiation from the skin to a thermal image. Due to higher metabolism, more heat will be produced in a tumour than in the surrounding healthy tissue. The heat can either be detected by a television tube or by liquid crystals that creates a temperature dependent colour on a self-developing film [8]. However, an abnormal

thermogram is not specific for cancer, but can also be found in acute inflammatory diseases. Studies indicate that the technique in detecting breast abnormalities is limited as is the diagnosis of already known, suspicious lesions [3].

2.7 Tomographic Methods

Tomography is a method to create three-dimensional images using X-rays, ultrasound or visible light. The object is then scanned in slices from different angles, giving one image for every scan. These images are then digitised and a computer can thus make a three-dimensional image of the object. To detect breast cancer this method can be used when performing light scanning. Some experiments using this method of enhancing the contrast have been performed on tissue phantoms with satisfactory results [6].

2.8 Methods Using Visible Light

The first attempt to transilluminate the breast in order to detect cancer was, as previously mentioned, performed by Ewing in 1928 [1]. Because the method was uncomfortable to the patient due to heat production, and the light intensity was low, the technique did not gain any general interest at that time. To make the examination more lenient to the patients, Cutler developed a method of water cooling in 1929 [2]. The method of just using a strong lamp was not successful, since it was not possible to distinguish tumours from other non-cystic structures. With the development of new equipment the idea of using visible light for screening has been reintroduced.

In 1972 Gros *et al.* introduced a technique called diaphanography, which uses photographic film as a detector. They used a very intense light source and discovered that light with longer wavelengths were more suitable for the transillumination of tissue [9].

This method was improved by Ohlsson *et al.* by introducing a highly sensitive infrared film to increase the contrast. They managed to detect 10 out of 11 malignant tumours among 1575 patients with this method [10].

If a video camera is used instead of the film, it is possible to digitise the image and to analyse it in a computer. Carlsen uses this technique when he illuminates the breast with light of two different wavelengths [11]. By digitising the two images obtained at the two different wavelengths a colour image showing areas with unusual absorption can be calculated. Since the tumour region has an elevated level of haemoglobin due to neovascularisation, these areas are considered possible tumours.

2.8.1 Time Resolved Methods

Multiple scattering of light causes a decreased contrast in the transmitted light and therefore prohibits visual observation inside turbid media, such as tissue. To suppress the

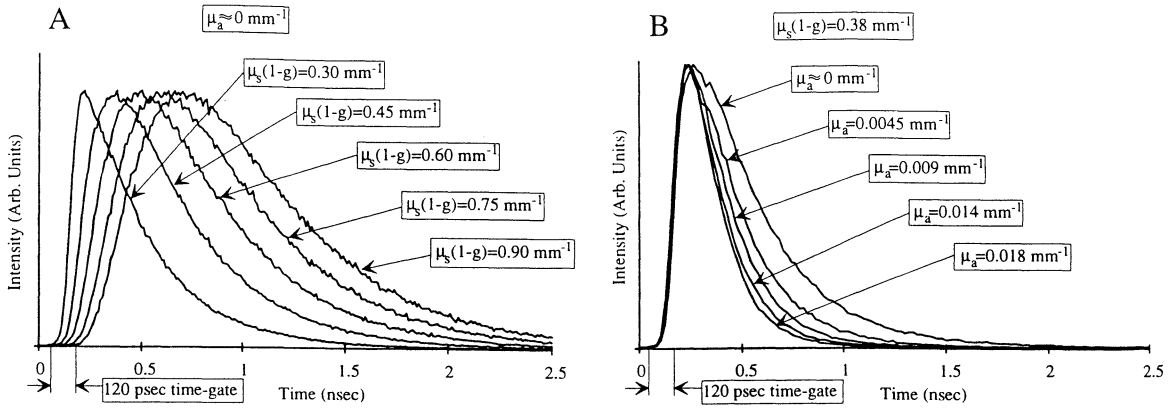

Fig. 1. *Time dispersion curves measured through a homogenous tissue phantom 30 mm thick.*
(A) *Fixed* μ_a *and varying* $\mu_s(1-g)$.
(B) *Fixed* $\mu_s(1-g)$ *and varying* μ_a.
(From Ref. [13].)

multiply scattered light and thus enhance the contrast in transillumination it is possible to use time-resolved detection. This technique is based on the concept that the medium is transilluminated with very short (picosecond) laser pulses, and the transmitted light is detected with time resolution. The light that leaves the turbid medium first travels a shorter path within the medium than the light exiting later. Thus, the intensity of the early light will depend on the optical properties of a volume close to a straight line through the medium.

The time-resolved detection can be achieved in several ways [12]. Optical streak cameras have good temporal resolution, but need rather high light levels to obtain a good signal-to-noise ratio. Optical Kerr gates and other non-linear optical shutters have high temporal resolution. Stimulated Raman amplification can also be used to create a time gate with high temporal resolution and high sensitivity. These techniques, however, need high power laser pulses to open the shutters.

Time-correlated single-photon counting is a technique where the time delay between the laser pulse and a detected photon is measured for a great number of pulses. Here the probability of detecting more than one photon per laser pulse must be negligible. The time dispersion curve will then be obtained by making a histogram of these delays (Fig. 1). This technique has the advantages of high sensitivity, but the temporal resolution is not that good. Using this time-correlated single-photon counting, Andersson-Engels *et al.* have shown, that the detection of transmitted light is practically insensitive to variations in the absorption coefficient [13]. To detect tumours in time-gated viewing it is the scattering coefficient of the tumour that must be characteristic (Fig. 2). One major drawback with these measurements, is the long sampling time. Since not more than one photon per laser pulse is detected, a lot of pulses are needed to make any statistics of the measured time delays. The scanning speed is typically 60 seconds per scanning point and the points are separated with 1 or 2 mm [13, 14].

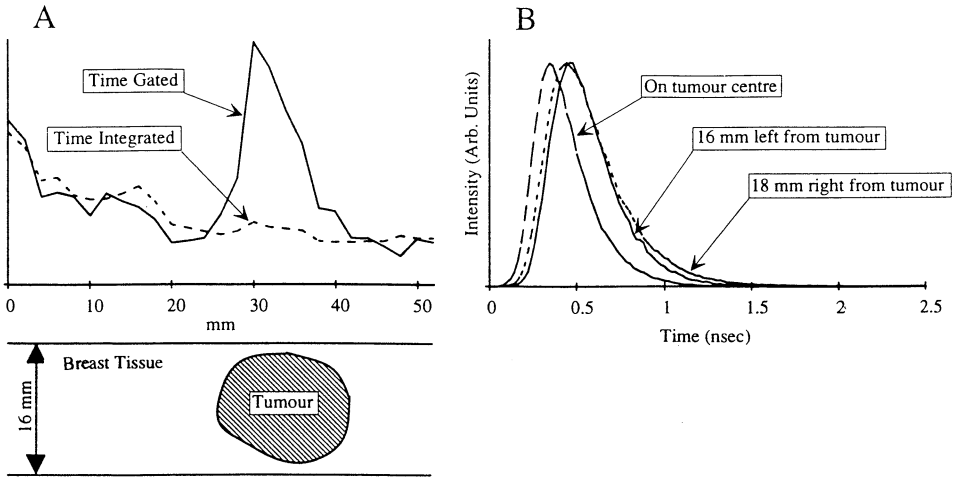

Fig. 2. (A) *A scan across a sample of breast tissue 16 mm thick containing a tumour 18 mm in diameter.* (B) *The corresponding time dispersion curves for three positions along the scan. (From Ref. [13].)*

2.8.2 PHASE RESOLVED METHODS

Phase-resolved and time-resolved methods are essentially equivalent. In Fig. 1 it is obvious that if an intensity-modulated light source irradiates a turbid medium, a phase shift due to the scattering properties of the sample will be found in the detected signal. This signal will also be demodulated due to absorption and scattering. In time-resolved methods, this can be seen as a broadening of the pulse (see Fig. 1).

Both the time-resolved and the phase-resolved techniques originate from fluorescence lifetime measurements. Phase-modulation fluorometers were constructed prior the development of the technology that made time resolved measurements possible. The use of these early phase-resolved fluorometers was limited since they only operated at one to three fixed frequencies (see e.g. [15]). With the development of pulsed lasers and fast detectors, time resolved techniques were to dominate. During the last decade, however, there has been a remarkable progress in the technique of frequency-domain fluorometry. In this method the frequency-dependent phase angle and modulation of the emission in response to intensity-modulated excitation are measured over a wide range of frequencies. The most common technique in phase-resolved measurements, is the cross-correlation detection. If the modulation frequency of the light source is ω then the detector is modulated at a frequency offset, $\omega + \Delta\omega$. The phase and modulation are measured on the low-frequency cross-correlation signal, $\Delta\omega$, which is typically below 50 Hz [15, 16]. The two closely spaced frequencies are provided by two frequency synthesisers, which are driven by the same crystal reference source and are thus phase-locked. This means that the relative stability of the synthesisers is improved.

The above mentioned technique has also been adopted for measuring the optical properties of a scattering medium. Fishkin *et al.* [17] have shown, that the absorption coefficient and the scattering coefficient can be calculated from measurements of the phase and the demodulation of the detected signal.

Different efforts have also been made to use this technique for localisation of absorbers in scattering media [18] and imaging of tissue [19]. Berndt *et al.* [18] used two fibre bundles to illuminate a cuvette with a scattering liquid, within which a black cylindrical rubber absorber was placed. The light was produced by a pulsed laser with a repetition frequency of 3.81 MHz. As a detector an image intensifier and a CCD-camera were used in a back-scattering arrangement. The gain of the image intensifier was modulated with a harmonic of the laser pulse repetition rate. Thus a steady-state image was obtained at the intensifier output screen. At least two images were taken under different image intensifier modulation conditions, such as modulation phase and modulation degree. By processing these images in a computer a final image can be created. In this image the contrast is based only on time differences of the back-scattered photons.

Gratton *et al.* [19] have also used the cross-correlation technique for imaging. A portion of porcine brain with an implanted black plastic button was scanned by moving two fibre bundles co-linearly. The average intensity, phase lag and modulation ratio were recorded at each position and were then presented as three three-dimensional diagrams (maps). In the intensity image no sign of the plastic button could be seen, but in the two others a sharp structure appeared.

2.9 THE PURPOSE OF THIS PROJECT

The purpose of this project was to construct a phase resolved transillumination equipment. One aspect was to use as simple and inexpensive equipment as possible. The idea is to use a low-power near-infrared laser diode as a light source. This laser diode is easily modulated with a sinusoidal signal from a frequency generator. The light that is transmitted through the tissue phantom is detected with an optical system. The output from the detector is mixed with the signal from the frequency generator. Since both signals are modulated with the same frequency, the output from the mixer is a DC level proportional to the cosine of the phase lag and an AC signal of the double frequency, which is not of interest.

With this technique only one frequency generator is needed, which lowers the cost drastically. Using a laser diode as a light source also lowers the costs, since there are many inexpensive diodes available in the near-infrared region. The modulation is also easy accomplished and demands no further optical components.

The goal was, as a first step, to make point measurements and to try to locate tumour phantoms within the tissue phantom. If this was successful, the next step would be to use this technique for scanning over the phantom to make an image of its contents.

3 THE INTERACTION OF LIGHT WITH TISSUE

Today most methods for the detection of breast cancer involve some kind of penetration of tissue by electromagnetic waves. The depth of penetration depends very much on the wavelength that is used. X-rays, which have a wavelength between 10^{-13} and 10^{-7} m, have a very good penetration capability. For visible light (≈ 400 to 700 nm), the penetration capability is very dependent on the wavelength. In Fig. 3 the diffuse transmittance for different kinds of tissue is shown as a function of the wavelength [20]. The diffuse transmittance is the fraction of the incident light that has passed through the tissue. It was measured with an incident beam of near monochromatic light and detected with an integrating sphere on the opposite side of the sample. In Fig. 4 the same kind of measurement is shown with a normal human breast *in vivo* as a sample [20]. The results show that suitable light for penetrating tissue is near-infrared light, that is light with a wavelength of 700 to 950 nm [e.g. 20].

3.1 REFLECTION

When light propagates through tissue there are three possibilities of interaction between light and tissue. The photons might either be reflected at the tissue surface, absorbed by the molecules in the tissue or scattered within the tissue.

Reflection occurs when light passes from one medium to another with different refractive indices, *n*. The polarisation and the angle of the incident light also affect the reflection.

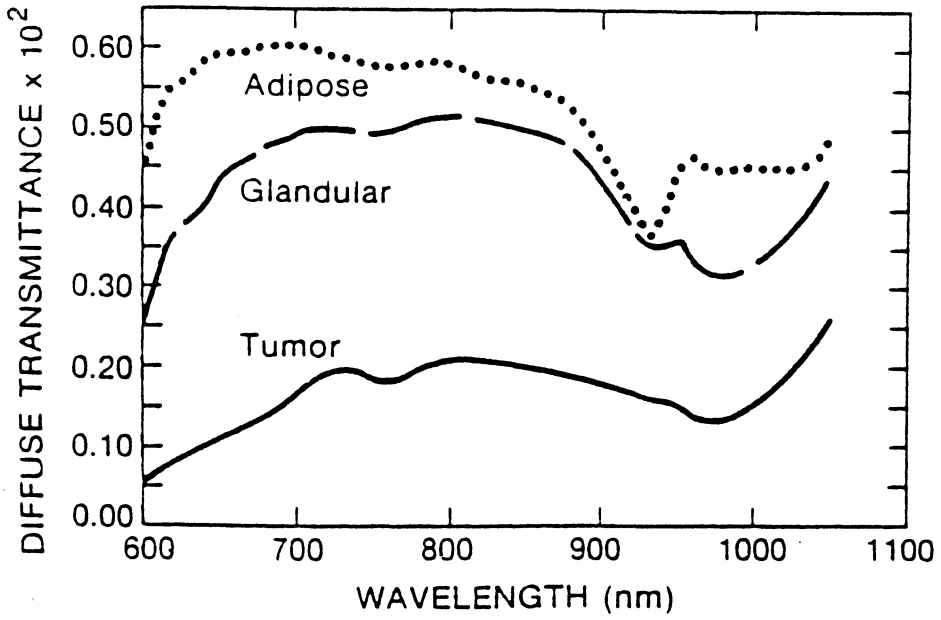

Fig. 3. *Diffuse transmittance versus wavelength for dissected breast tissue. Measurements were made within 8h of removal of tissue from body. (From Ref. [20].)*

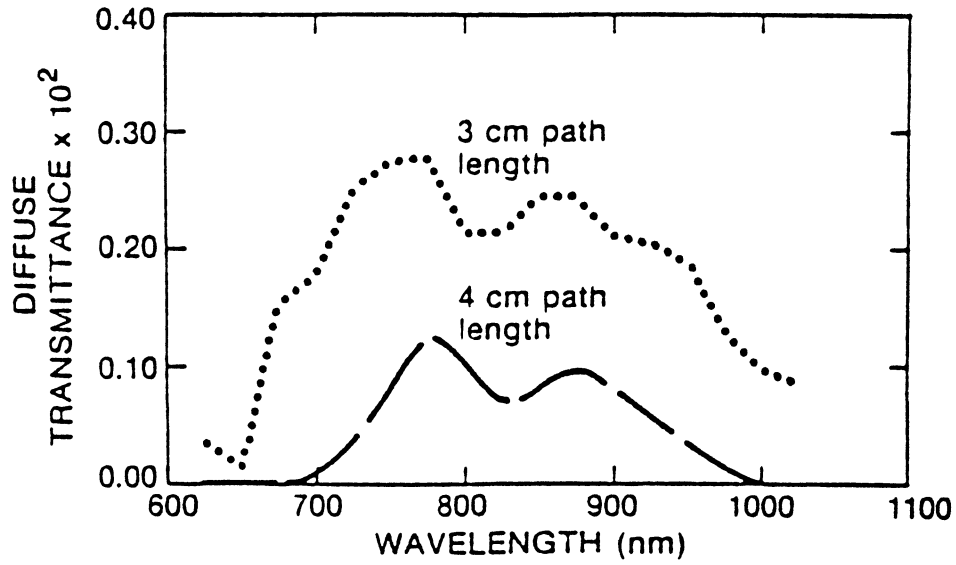

Fig. 4. In vivo *measurements of diffuse transmittance for intact nonmalignant human breast. From reference [20].*

The fraction of light that is reflected is called the reflectance, R. Assume that light passes from one medium with the refractive index n_1 to another medium with refractive index n_2. Then the reflectance will be

$$R_{\perp} = \left(\frac{n_1 \cos\theta_1 - n_2 \cos\theta_2}{n_1 \cos\theta_1 + n_2 \cos\theta_2} \right)^2$$

$$R_{//} = \left(\frac{n_2 \cos\theta_1 - n_1 \cos\theta_2}{n_2 \cos\theta_1 + n_1 \cos\theta_2} \right)^2$$

Here $R_{\perp}$ and $R_{//}$ is the reflectance of light polarised perpendicularly and parallel to the incident plane, respectively. Further, θ_1 is the angle of incidence and θ_2 is the angle of transmission given by Snell's law:

$$n_1 \sin\theta_1 = n_2 \sin\theta_2$$

The main constituent of the human body, water, has a refractive index of 1.33, while the refractive index of fat and concentrated proteins is approximately 1.55. This difference causes reflection, not only at the boundary of the tissue, the skin, but also within the

tissue. When light passes from air to tissue at normal incidence, about 2-4% of the light is reflected.

The fraction of light that is not reflected at the boundary enters the tissue and is thus transmitted into it. If there is no absorption or scattering at the boundary, the transmission, T, is:

$$T_{\perp} = 1 - R_{\perp}$$
$$T_{//} = 1 - R_{//}$$

As for the reflectance, $T_{\perp}$ and $T_{//}$ denote perpendicular and parallel polarisation of the transmittance, respectively.

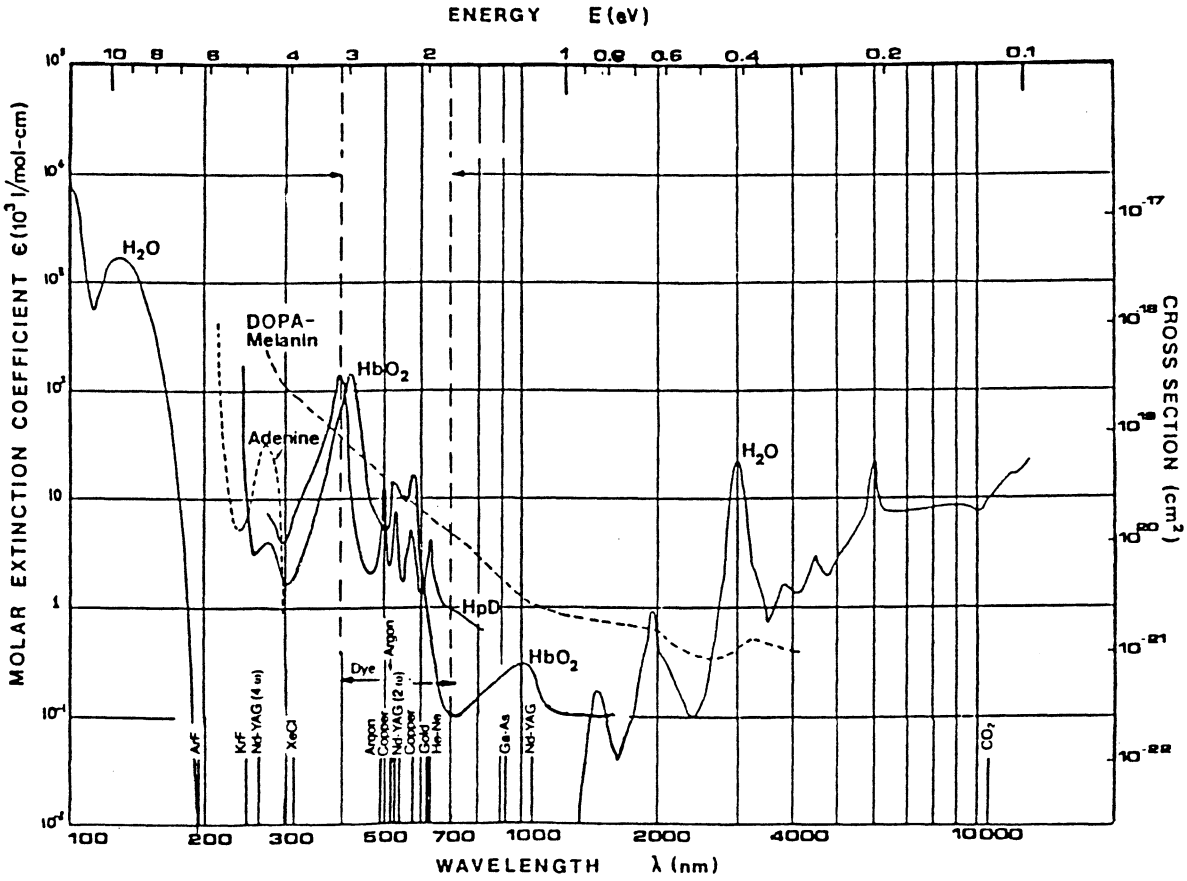

Fig. 5. *Molecular extinction coefficient for a number of tissue constituents and haematoporphyrin derivate as a function of wavelength. The wavelengths of the most frequently used medical lasers are indicated. (From Ref. [21].)*

3.2 ABSORPTION

If a turbid medium is irradiated with laser light, the radiance inside the tissue can be divided into a coherent part, I_c, and a diffuse part I_d, where $I = I_c + I_d$. The coherent part is the direct light and has not yet interacted with the tissue. Thus, the attenuation will simply follow the Beer-Lambert law,

$$I_c(x) = I_c(0)\mathrm{e}^{-\mu_a x}.$$

Here I is the intensity after a distance x and μ_a is the absorption coefficient. A useful quantity is the mean free path of the coherent light, which is defined as $\delta = 1/\mu_a$. When a photon from the coherent light interacts with the medium, it will either be absorbed and dissappear or it will be scattered and change status to be included in the diffuse scattered light. Scattering will be furhter described in chapter 3.3.

The three main absorbers in tissue for light with a wavelength larger than 300 nm have been determined to be water, haemoglobin and melanin [24]. Their absorption spectra are shown in Fig. 5. Below 300 nm most molecules absorb. As can be seen in the Fig. 5 and Fig. 6, tissue is most transparent if the wavelength is between 620 nm and 1.3 μm. In that region the attenuation coefficient varies typically from 2.5 to 5 cm^{-1}. That means that the intensity decreases with a factor e^{-1} after 0.4 to 0.2 cm. If blue light is used, the attenuation coefficient rises to 20 cm^{-1} and for ultraviolet or infrared light with a wavelength greater than 2.5 μm it will be between 100 and 300 cm^{-1}.

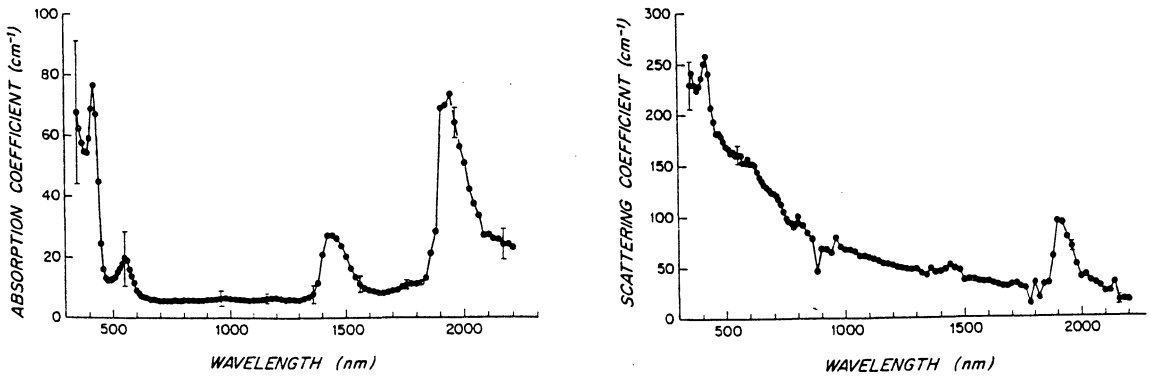

Fig. 6. *Average values of* a) *tissue absorption coefficient, and* b) *tissue scattering coefficients, of a rat liver* in vitro *as a function of wavelength. Vertical bars represent one standard deviation from recordings of 11 samples. (From Ref. [22].)*

3.3 SCATTERING

Due to the high absorption coefficient in the ultraviolet, blue and far infrared wavelength regions, only red or near infrared light can be used for tissue transillumination. Scattering will be the main process to determine the penetration depth. This is clearly shown in Fig. 6, which presents the spectral variations of the absorbtion coefficient and the scattering coefficient of a rat liver *in vitro*. In the region between 650 nm and 1300 nm, where the absorbtion coefficient is about 5 cm^{-1}, the scattering coefficient varies from 150 cm^{-1} to 50 cm^{-1}. This corresponds to a variation in the mean free path from 70 μm to 200 μm.

Any incident photon will, after a short distance, lose its original direction due to scattering in the turbid medium. The electric field of the photon causes the electrons of the encountered atom or molecule to oscillate and the particle acts as a "light source" itself and can emit the photon in another direction with the same or less energy as it had before the collision. There are different types of scattering depending on the size of the scattering particle.

If the scattering particle is very small compared to the wavelength of the light, Rayleigh or Raman scattering can occur. Then the scattered light is weak, polarised and almost isotropic. The scattering probability is proportional to $1/\lambda^4$, where λ is the wavelength. Thus blue light is more likely to be scattered than red light. Rayleigh scattering is an elastic process where the scattered photon has gets the same energy as the incident photon. If the photon is Raman scattered, on the other hand, it looses energy.

If the scattering object is larger than the wavelength of the light, an elastic form of scattering, named Mie scattering, occurs. The relative cross section for Mie scattering is a complicated function of the wavelength, the particle radius, refractive indices and absorption. The intensity of the scattered light is approximately proportional to $1/\lambda^2$.

Finally, internal reflection, i.e. reflections inside the particle due to variations in the refractive indices, can also contributes to the scattering. All these scattering processes make the incident photons loose their original directions after a very short distance and thus the photon transport can be described as a diffusion process. This means that the contrast in tissue transillumination will be poor.

3.4 THEORETICAL MODELS

Exact modelling of light distribution in tissue during light irradiation is not possible since the tissue is not homogenous. As mentioned above, local variations in the refractive index of the tissue causes strong scattering. The angular distribution of the scattered light is not necessarily isotropic, and the intensity can be higher in certain directions than in others. Furthermore, the inhomogenity of tissue with boundaries between different tissue types, will prohibit microscopically accurate solutions. Assumptions of the optical properties must be made and a macroscopical light distribution within the tissue can then be modelled. The models can be based on either fundamental microscopic or macroscopic

optical coefficients. To handle these multiple scattering problems theoretically, two distinct types of theories have been developed [23]. One may be called analytical theory and the other transport theory.

In the analytical theory the fundamental relationship is Maxwell's equations or the wave equation. The scattering and absorption characteristics of the tissue are inserted and differential or integral equations are obtained. In practice, however, it is impossible to formulate a problem that completely includes all effects and the calculations get very complex.

Transport theory on the other hand, deals directly with the transport of energy. Correlation effects between the different electromagnetic fields, such as diffraction and interference, are neglected and therefore the addition of powers rather than the addition of fields holds. Transport theory has been successfully used in a large number of physical applications, such as neutron diffusion, radiative transfer, the theory of plasmas and the theory of sound propagation. Using transport theory, light fluency can be calculated in two different ways, either by solving the transport equation or by Monte Carlo simulations of the light distribution.

In this paper the transport equation will be discussed. Solving the transport equation is probably the most often used method to model the light distribution in tissue [24].

3.4.1 Linear Transport Theory

To describe the particle distribution a few definitions must be made. (The following definitions are adopted from Case *et al.* [25].) Since the particles of interest are photons, assume that there are no forces and therefore no collisions between them. Hence they behave much as an ideal gas. Their distribution is completely specified by the single-particle distribution function $\psi(\mathbf{r},\mathbf{v},t)$, which is also called angular density.

Definition 1. $\psi(\mathbf{r},\mathbf{v},t)d^3rd^3v$ is the expected number of particles in the volume element d^3r about the point $\mathbf{r}$, whose velocities lie in the element of velocity space d^3v about $\mathbf{v}$, at time t.

When the one-speed approximation is made, the speeds of the particles are not as interesting as the direction of the velocity, which can be described by a unit vector $\mathbf{\Omega}$.

Definition 2. $\mathbf{\Omega} = \mathbf{v}/v$, where v is the speed of the particle. Then $d^3v = v^2 dv d\mathbf{\Omega}$

Related to the angular density is the angular current, $\mathbf{j}(\mathbf{r},\mathbf{v},t)$.

Definition 3. $\mathbf{j}(\mathbf{r},\mathbf{v},t) = \mathbf{v}\psi(\mathbf{r},\mathbf{v},t)$.

Another, equivalent, definition of the angular current is

Definition 3'. $\mathbf{j}(\mathbf{r},\mathbf{v},t)\cdot\mathbf{n}dSd^3vdt$ is the number of particles in d^3v about $\mathbf{v}$ which cross a small area dS with unit normal $\mathbf{n}$ in a time dt.

Also related to the angular density are the energy-dependent density, $\rho(\mathbf{r},v,t)$, and the density, $\rho(\mathbf{r},t)$.

Definition 4. a) $\rho(\mathbf{r},v,t)=\int\psi(\mathbf{r},\mathbf{v},t)d\Omega$,

b) $\rho(\mathbf{r},t)=\int\psi(\mathbf{r},\mathbf{v},t)d^3v$.

From definition 4 it is obvious that $\rho(\mathbf{r},t)d^3r$ represents the total number of particles in d^3r at $\mathbf{r}$, independent of their velocity while $\rho(\mathbf{r},\ v,\ t)d^3rv^2dv$ represents the total number of particles in d^3r with speeds between v and $v+dv$ independent of the direction of their velocities.

Likewise, the currents $\mathbf{J}(\mathbf{r},v,t)$ and $\mathbf{J}(\mathbf{r},t)$ may be defined by integrating $\mathbf{j}(\mathbf{r},\mathbf{v},t)$ over $d\Omega$ and over d^3v, respectively. The net number of particles crossing dS in time dt is then given by $\mathbf{J}(\mathbf{r},\mathbf{v},t)\cdot\mathbf{n}dSdt$.

Particles inserted into the medium by sources that are independent of the particle population present may be described by an angular source density.

Definition 5. $q(\mathbf{r},\ \mathbf{v},\ t)d^3rd^3vdt$ is the number of particles inserted into d^3r at $\mathbf{r}$ and d^3v at $\mathbf{v}$ between t and $t+dt$.

The quantities $q(\mathbf{r},v,t)$ and $q(\mathbf{r},t)$ may also be defined by integration of $q(\mathbf{r},\ \mathbf{v},\ t)$ over $d\Omega$ over d^3v, respectively.

Definition 6. $\mu_t(\mathbf{r},\mathbf{v})$ is the inverse mean free path, which also is called the macroscopic cross-section, of a particle at $\mathbf{r}$ and with a speed $\mathbf{v}$.

A particle of velocity $\mathbf{v}$ will suffer, on the average, $v\mu_t$ interactions with the surrounding medium per second. The collision rate for particles of velocity $\mathbf{v}$ at $\mathbf{r}$ will thus be $v\mu_t(\mathbf{r},\mathbf{v})\psi(\mathbf{r},\mathbf{v},t)d^3rd^3v$

When discussing light propagation through turbid media, $\mu_t(\mathbf{r},\mathbf{v})$ is the sum of the scattering coefficient, μ_s, and the absorption coefficient, μ_a

$$\mu_t(\mathbf{r},\mathbf{v})=\mu_s(\mathbf{r},\mathbf{v})+\mu_a(\mathbf{r},\mathbf{v}) \tag{1}$$

Whenever a particle interacts with the medium, $c(\mathbf{r},\mathbf{v})$ secondary particles will result.

Definition 7. $c(\mathbf{r},\mathbf{v})$ is the average number of secondary particles per collision produced at $\mathbf{r}$ by a particle of velocity $\mathbf{v}$.

Clearly, for a scattering collision $c = 1$ and for an absorption collision $c = 0$. In this application c might also be recognised as the albedo, a, which is the ratio between the scattering coefficient and the total attenuation coefficient;

$$c(\mathbf{r},\mathbf{v}) = \frac{\mu_s(\mathbf{r},\mathbf{v})}{\mu_s(\mathbf{r},\mathbf{v}) + \mu_a(\mathbf{r},\mathbf{v})} = a \tag{2}$$

Finally, there is only one more function to define, $\mu_t(\mathbf{v}' \rightarrow \mathbf{v},\mathbf{r})$

Definition 8. $v'\mu_t(\mathbf{v}' \rightarrow \mathbf{v},\mathbf{r})\psi(\mathbf{r},\mathbf{v}',t)d^3v'd^3rd^3vdt$ is the probable number of particles in d^3r at $\mathbf{r}$ emitted into d^3v at $\mathbf{v}$ in time dt about t, induced by particles of velocity in d^3v' at $\mathbf{v}'$.

In definition 8 the approximation that particles produced by interaction appear at the same point and time as the interaction. Then definitions 6, 7 and 8 give

$$\int \mu_t(\mathbf{v}' \rightarrow \mathbf{v},\mathbf{r})d^3v = c(\mathbf{r},\mathbf{v}')\mu_t(\mathbf{r},\mathbf{v}') \tag{3}$$

3.4.2 THE TRANSPORT EQUATION

A simple derivation of the transport equation may start from a balance equation based on conservation of particles within a small volume element of phase space [25]. Consider the change dN in time dt of the number of particles with velocity in d^3v about $\mathbf{v}$ that are located in a small volume V with surface S about the point $\mathbf{r}$. Mathematically, this can be written as

$$dN = d^3vdt\int_V \frac{\partial\psi(\mathbf{r},\mathbf{v},t)}{\partial t}d^3r \tag{4}$$

However, the change dN can also be expressed as a balance equation

$dN =$ - (a) net number flowing out of S in dt (5)
- (b) number suffering collisions in V in dt
+ (c) number of secondaries of velocity $\mathbf{v}$ produced in V in dt by collisions
+ (d) number of particles of velocity $\mathbf{v}$ produced in V in dt by sources.

Particles that enter and leave the volume element V with no change in velocity are included in term (a), while particles that enter and leave the velocity space element d^3v with no change in position are included in terms (b) and (c), respectively. The four terms of the balance equation must now be expressed mathematically. Term (a) is expressed in the definitions as

$$(a) = d^3v dt \int_S \mathbf{j}(\mathbf{r},\mathbf{v},t)\cdot\mathbf{n}_0 dS,$$

where $\mathbf{n}_0$ is the outward normal to dS. This is now an integral over the surface of the volume, while Eq. (4) is an integral over the volume itself. To get both equations on the same form, Gauss's theorem is applied on (a) which then is transformed to

$$(a) = d^3v dt \int_V \nabla\cdot\mathbf{j} d^3r$$

Among the definitions it can also be found that

$$(b) = d^3v dt \int_V v\mu_t(\mathbf{r},\mathbf{v})\psi(\mathbf{r},\mathbf{v},t)d^3r$$

$$(c) = d^3v dt \iint_V v'\psi(\mathbf{r},\mathbf{v}',t)\mu_t(\mathbf{v}'\rightarrow\mathbf{v},\mathbf{r})d^3v'd^3r$$

$$(d) = d^3v dt \int_V q(\mathbf{r},\mathbf{v},t)d^3r$$

If Eq. (4) and Eq. (5) are combined, upon noting that the volume V is arbitrary, they yield

$$\frac{\partial\psi(\mathbf{r},\mathbf{v},t)}{\partial t} + \mathbf{v}\cdot\nabla\psi(\mathbf{r},\mathbf{v},t) + v\mu_t(\mathbf{r},\mathbf{v})\psi(\mathbf{r},\mathbf{v},t) = \tag{6}$$

$$= q(\mathbf{r},\mathbf{v},t) + \int \mu_t(\mathbf{v}'\rightarrow\mathbf{v},\mathbf{r})v'\psi(\mathbf{r},\mathbf{v}',t)d^3v'$$

To get Eq. (6), the common differentials have been cancelled. The identity $\nabla\cdot\mathbf{v}\psi = \mathbf{v}\cdot\nabla\psi$, which is true since $\mathbf{v}$ is an independent variable, has also been used.

Eq. (6) is the fundamental transport equation for particles. Written as above, it is usually very difficult to handle. Therefore, a few assumptions and approximations will have to be made.

3.4.3 THE ONE-SPEED APPROXIMATION

The linear transport equation describes a balance of particles that flow in a certain element of volume. It takes into account their velocity, position and changes of these variables due to collisions. Since photons all travel with the same speed in a small element of volume, the function $\mu_t(\mathbf{v}' \rightarrow \mathbf{v}, \mathbf{r})$ can be written in the form

$$\mu_t(\mathbf{v}' \rightarrow \mathbf{v}, \mathbf{r}) = \mu_t(\Omega' \cdot \Omega, \mathbf{r}, v)\frac{\delta(v - v')}{v^2} \tag{7}$$

in which case

$$\mu_t(\mathbf{r}, v)c(\mathbf{r}, v) = \int \mu_t(\Omega' \cdot \Omega, \mathbf{r}, v)d\Omega = \int \mu_t(\Omega' \cdot \Omega, \mathbf{r}, v)d\Omega'. \tag{8}$$

To make the calculations more convenient a new function $f(\Omega' \cdot \Omega, \mathbf{r}, v)$, defined by

$$f(\Omega' \cdot \Omega, \mathbf{r}, v) = \frac{\mu_t(\Omega' \cdot \Omega, \mathbf{r}, v)}{c(\mathbf{r}, v)\mu_t(\mathbf{r}, v)} \tag{9}$$

is introduced. From Eq. (8) and (9) it is obvious that $f(\Omega' \cdot \Omega, \mathbf{r}, v)$ is normalised to unity.

Using the equalities above the one-speed linear transport equation will be

$$\frac{\partial \psi(\mathbf{r}, \Omega, t)}{\partial t} + v\Omega \cdot \nabla \psi(\mathbf{r}, \Omega, t) + v\mu_t(\mathbf{r}, v)\psi(\mathbf{r}, \Omega, t) = \tag{10}$$

$$= q(\mathbf{r}, \Omega, t) + v\mu_t(\mathbf{r}, v)c(\mathbf{r}, v)\int \psi(\mathbf{r}, \Omega', t)f(\Omega' \cdot \Omega, \mathbf{r}, v)d\Omega'$$

3.4.4 THE DIFFUSION APPROXIMATION

To solve the one-speed linear transport equation the spherical-harmonics method is used [25]. The basic idea of this method is very simple: the spherical-harmonics expansion of $\psi(\mathbf{r}, \Omega, t)$ as well as a similar expansion of $q(\mathbf{r}, \Omega, t)$ are introduced into the transport equation. The expansions might be written as

$$\psi(\mathbf{r}, \Omega, t) = \sum_{l=0}^{\infty} \sum_{m=-l}^{l} \sqrt{\frac{2l+1}{4\pi}} \psi_{lm}(\mathbf{r}, t)Y_{lm}(\Omega) \tag{11a}$$

$$q(\mathbf{r},\Omega,t)=\sum_{l=0}^{\infty}\sum_{m=-l}^{l}\sqrt{\frac{2l+1}{4\pi}}q_{lm}(\mathbf{r},t)Y_{lm}(\Omega) \tag{11b}$$

In addition, $f(\Omega'\cdot\Omega)$ is expanded in terms of a series of Legendre polynomials:

$$f(\Omega'\cdot\Omega)=\sum_{l=0}^{\infty}\frac{2l+1}{4\pi}f_l P_{lm}(\Omega'\cdot\Omega)=\sum_{l=0}^{\infty}\sum_{m=-l}^{l}\sqrt{\frac{2l+1}{4\pi}}f_l Y_{lm}^{*}(\Omega')Y_{lm}(\Omega) \tag{11c}$$

If these expansions are substituted into the Eq. (10), and if the resulting equation is multiplied by $Y_{lm}^{*}(\Omega)$ and integrated over Ω, an infinite coupled set of differential equations in the unknown ψ_{lm} is obtained.

The so-called diffusion approximation is, at least for the one-speed case discussed here, simply the lowest-order spherical-harmonics approximation. In other words, the sum over l in Eq. (11) includes only those terms with $l = 0$ and 1. That is, we have

$$\psi(\mathbf{r},\Omega,t)\approx\sqrt{\frac{1}{4\pi}}\psi_{00}(\mathbf{r})Y_{00}(\Omega)+\sqrt{\frac{3}{4\pi}}\sum_{m=-1}^{1}\psi_{1m}(\mathbf{r})Y_{1m}(\Omega) \tag{12}$$

If this expansion, and the expansions of $q(\mathbf{r},\Omega,t)$ and $f(\Omega'\cdot\Omega)$, are inserted into the transport equation and the intergration is carried out, the result will be four equations for the four unknown ψ_{lm}. However, it is much more convenient to proceed as follows.

Since $Y_{00}=1/\sqrt{4\pi}$ is a scalar and since the Y_{1m} are the three components of a vector, Eq. (12) may be rewritten in the form

$$\psi(\mathbf{r},\Omega,t)=A+\Omega\cdot\mathbf{B} \tag{13}$$

To determine A, Eq. (13) is first integrated over Ω

$$\int\psi(\mathbf{r},\Omega,t)d\Omega=\int(A+\Omega\cdot\mathbf{B})d\Omega. \tag{14a}$$

Using definition 4a and observing that $\int\Omega\cdot\mathbf{B}d\Omega=0$, an expression for A will be obtained,

$$A=\frac{1}{4\pi}\rho(\mathbf{r},t) \tag{14b}$$

To determine **B**, Eq. (13) is multiplied with Ω before the integration is carried out,

$$\int \Omega\psi(\mathbf{r},\Omega,t)d\Omega = \int \Omega(A+\Omega\cdot\mathbf{B})d\Omega, \tag{15a}$$

which results in

$$\mathbf{B} = \frac{3}{4\pi v}\mathbf{J}(\mathbf{r}). \tag{15b}$$

To get Eq. (15b), defintion 3 is combined with the facts that

$$\int A\Omega d\Omega = 0 \tag{16a}$$

and

$$\int \Omega(\mathbf{B}\cdot\Omega)d\Omega = \frac{4\pi}{3}\mathbf{B}. \tag{16b}$$

Thus the expansion of the angular density becomes, in this approximation,

$$\psi(\mathbf{r},\Omega,t) = \frac{1}{4\pi}\left(\rho(\mathbf{r},t)+\frac{3}{v}\mathbf{J}(\mathbf{r},t)\cdot\Omega\right). \tag{17}$$

In a similar way, the expansion of the angular dependence of the source, $q(\mathbf{r},\Omega,t)$ might be written as

$$q(\mathbf{r},\Omega,t) = \frac{1}{4\pi}\left(q_0(\mathbf{r},t)+3\mathbf{q}_1(\mathbf{r},t)\cdot\Omega\right) \tag{18}$$

Inserting Eq. (17) and (18) into Eq. (10) gives, upon cancelling a common factor of 1/4π:

$$\frac{\partial\rho}{\partial t}+\frac{3}{v}\frac{\partial(\mathbf{J}\cdot\Omega)}{\partial t}+v\Omega\cdot\nabla\left(\rho+\frac{3}{v}\mathbf{J}\cdot\Omega\right)+v\mu_t\left(\rho+\frac{3}{v}\mathbf{J}\cdot\Omega\right)= \tag{19}$$

$$=\left(q_0+3\mathbf{q}_1\cdot\Omega\right)+v\mu_t c\int\left(\rho+\frac{3}{v}\mathbf{J}\cdot\Omega'\right)f(\Omega'\cdot\Omega)d\Omega'.$$

The integral on the right-hand side of Eq. (19) may be performed by noting that

$$\int f(\Omega' \cdot \Omega) d\Omega' = 1 \tag{20a}$$

and

$$\int \Omega' f(\Omega' \cdot \Omega) d\Omega' = \alpha \Omega, \tag{20b}$$

where α is a constant to be determined. This can be done by taking the scalar product of Eq. (20b) with Ω. Since $\Omega \cdot \Omega = 1$, this will give

$$\alpha = \int (\Omega \cdot \Omega') f(\Omega' \cdot \Omega) d\Omega' \equiv g, \tag{21}$$

where g is the average of the cosine of the scattering angle. Eq. (19) is thus reduced to

$$\frac{1}{v}\frac{\partial \rho}{\partial t} + \frac{3}{v^2}\frac{\partial (\mathbf{J} \cdot \Omega)}{\partial t} + \{\Omega \cdot \nabla + (1-c)\mu_t\}\rho + \tag{22}$$

$$+\{\Omega \cdot \nabla + (1-cg)\mu_t\}\frac{3}{v}\mathbf{J} \cdot \Omega = \frac{1}{v}(q_0 + 3\mathbf{q}_1 \cdot \Omega).$$

This equation is reduced to two equations in the two dependent variables $\rho(\mathbf{r},t)$ and $\mathbf{J}(\mathbf{r},t)$ by integration over Ω. First, integrating Eq. (22) over Ω and making use of the fact that for arbitrary vectors **A** and **B**,

$$\int \Omega \cdot \mathbf{A} d\Omega = 0 \tag{23a}$$

and

$$\int (\Omega \cdot \mathbf{A})(\Omega \cdot \mathbf{B}) d\Omega = \frac{4\pi}{3}(\mathbf{A} \cdot \mathbf{B}), \tag{23b}$$

the following equation is obtained:

$$\frac{\partial \rho(\mathbf{r},t)}{\partial t} + v\{1 - c(\mathbf{r})\}\mu_t(\mathbf{r})\rho(\mathbf{r},t) + \nabla \cdot \mathbf{J}(\mathbf{r},t) = q_0(\mathbf{r},t) \tag{24}$$

Next, Eq. (22) is multiplied by Ω before the integration is made. Observing that

$$\int \Omega(\Omega \cdot \mathbf{A}) d\Omega = \frac{4\pi}{3}\mathbf{A} \tag{25a}$$

and

$$\int \Omega(\Omega \cdot \mathbf{A})(\Omega \cdot \mathbf{B}) d\Omega = 0, \tag{25b}$$

the resulting equation will be

$$\frac{1}{3}\nabla\rho(\mathbf{r},t) + \frac{1}{v^2}\frac{\partial \mathbf{J}(\mathbf{r},t)}{\partial t} + \frac{1}{3vD(\mathbf{r})}\mathbf{J}(\mathbf{r},t) = \frac{1}{v}\mathbf{q}_1(\mathbf{r},t). \tag{26}$$

Here $D(\mathbf{r})$ is the diffusion coefficient and is defined as

$$D(\mathbf{r}) = \frac{1}{3\mu_t(\mathbf{r})(1 - c(\mathbf{r})g)} \tag{27}$$

In this study, the particles that are being treated in the transport theory, are photons. Therefore, the average number of secondary particles per collision, c, might be replaced with the albedo, a, according to Eq. (2). Doing so, Eq. (27) may be rewritten as

$$D(\mathbf{r}) = \frac{1}{3(\mu_a(\mathbf{r}) + (1-g)\mu_s(\mathbf{r}))} \tag{28}$$

3.4.5 Isotropic Sinusoidally Modulated Point Source

Fishkin *et al.* have verified the validity of the diffusion approximation to the linear transport equation with a sinusoidally intensity modulated point source in a very turbid medium [18]. Mathematically, an isotropic point source of light that is sinusoidally intensity-modulated is described by:

$$q_0(\mathbf{r},t) = \delta(\mathbf{r})S(1 + A\exp[-i(\omega t + \varepsilon)]) \tag{29a}$$

$$\mathbf{q}_1(\mathbf{r},t) = 0 \tag{29b}$$

where $\delta(\mathbf{r})$ is a Dirac-delta function located at the origin, S is the source strength (in units of photons per second), A is the modulation amplitude of the source, $i = \sqrt{-1}$, ω is the angular modulation frequency and ε is an arbitrary phase.

Consider the case in which the system to be studied has uniform scattering, uniform absorption and isotropic scattering. That can be expressed as

$$\begin{aligned} \mu_t(\mathbf{r}) &= \text{constant} \\ a(\mathbf{r}) &= \text{constant} \\ g &= 0 \end{aligned}$$

With these assumptions, the diffusion coefficient is given by

$$D(\mathbf{r}) = \frac{1}{3\mu_t} = \text{constant} \tag{30}$$

Substituting Eq. (29) and (30) into the basic equations of diffusion theory, Eq. (24) and (26), and assuming that the solutions of the resulting equation have the form

$$\rho(\mathbf{r},t) = \rho_1(\mathbf{r}) + \rho_2(\mathbf{r})\exp(-i(\omega t + \varepsilon)) \tag{31a}$$

$$\mathbf{J}(\mathbf{r},t) = \mathbf{J}_1(\mathbf{r}) + \mathbf{J}_2(\mathbf{r})\exp(-i(\omega t + \varepsilon)), \tag{31b}$$

Eq. (24) and (26) may be separated in one steady-state part and one frequency dependent part. The steady-state equations are

$$v(1-a)\mu_t\rho_1(\mathbf{r}) + \nabla\cdot\mathbf{J}_1(\mathbf{r}) = S\delta(\mathbf{r}) \tag{32a}$$

$$\mathbf{J}_1(\mathbf{r}) = -\frac{v}{3\mu_t}\nabla\rho_1(\mathbf{r}), \tag{32b}$$

while the frequency dependent equations are expressed as

$$-i\omega\rho_2 + v(1-a)\mu_t\rho_2(\mathbf{r}) + \nabla\cdot\mathbf{J}_2(\mathbf{r}) = SA\delta(\mathbf{r}) \tag{33a}$$

$$\mathbf{J}_2(\mathbf{r}) = -\frac{v}{3\mu_t}\left(\frac{1+i\omega/v\mu_t}{1+(\omega/v\mu_t)^2}\right)\nabla\rho_2(\mathbf{r}). \tag{33b}$$

Since photons have a speed of $v \approx 10^{11}$ mm/s and the modulation frequency used in this study is $\omega \approx 10^{9}$ rad/s and the total attenuation coefficient $\mu_t \approx 1$ mm^{-1}, the following approximation can be made

$$\mathbf{J}_2(\mathbf{r}) \approx -\frac{v}{3\mu_t}\nabla\rho_2(\mathbf{r}). \tag{34}$$

If Eq. (32b) and (34) are inserted into Eq. (32a) and (33a), respectively, two differential equations for the components of $\rho(\mathbf{r})$ are obtained

$$-\Delta\rho_1(\mathbf{r}) + 3\mu_t^2(1-a)\rho_1(\mathbf{r}) = \frac{3\mu_t}{v}S\delta(\mathbf{r}). \tag{35}$$

$$-\Delta\rho_2(\mathbf{r}) + \left(3\mu_t^2(1-a) - i\frac{3\mu_t\omega}{v}\right)\rho_2(\mathbf{r}) = \frac{3\mu_t}{v}SA\delta(\mathbf{r}). \tag{36}$$

Here Δ is the Laplacian operator, $\nabla\cdot\nabla$. Assume that the two components of the angular density are on the form

$$\rho_i(\mathbf{r}) = \frac{\alpha_i}{r}e^{-\beta_i r}, \tag{37}$$

where α_i and β_i are constants.

If Eq. (37) is inserted into Eq. (35), using the facts that

$$\Delta\left(\frac{1}{r}e^{-\beta_i r}\right) = \left(\Delta\frac{1}{r}\right)e^{-\beta_i r} + \frac{1}{r}\left(\Delta e^{-\beta_i r}\right) + 2\frac{\partial}{\partial r}\left(\frac{1}{r}\right)\frac{\partial}{\partial r}\left(e^{-\beta_i r}\right), \tag{38a}$$

$$\Delta\left(\frac{1}{r}\right) = -4\pi\delta(\mathbf{r}) \text{ and} \tag{38b}$$

$$\Delta\left(e^{-\beta_i r}\right) = \left(\beta_i^2 - \frac{2\beta_i}{r}\right)e^{-\beta_i r}, \tag{38c}$$

the following equations will be obtained

$$4\pi\delta(\mathbf{r})\alpha_1 e^{-\beta_1 r} - \left(\beta_1^2 - 3\mu_t^2(1-a)\right)\frac{\alpha_1}{r}e^{-\beta_1 r} = \frac{3\mu_t}{v}S\delta(\mathbf{r}). \tag{39}$$

Remembering that $\delta(\mathbf{r})e^{-\beta_i r} = \delta(\mathbf{r})e^0 = \delta(\mathbf{r})$, the following identification can be done:

$$4\pi\delta(\mathbf{r})\alpha_1 = \frac{3\mu_t}{v} S\delta(\mathbf{r}) \tag{40a}$$

$$\beta_1^2 - 3\mu_t^2(1-a) = 0. \tag{40b}$$

From Eq. (40), the constants α_1 and β_1 can be determined

$$\alpha_1 = \frac{3\mu_t S}{4\pi v} \tag{41a}$$

$$\beta_1 = \mu_t\sqrt{3(1-a)}. \tag{41b}$$

This results in the following expression

$$\rho_1(\mathbf{r}) = \frac{3\mu_t S}{4\pi v}\exp\left(-r\mu_t\sqrt{3(1-a)}\right). \tag{42}$$

In a similar way Eq. (37) may be inserted in Eq. (36) to determine the second component of the angular component. The equations corresponding to (40a) and (40b) will then be

$$4\pi\delta(\mathbf{r})\alpha_2 = \frac{3\mu_t}{v} SA\delta(\mathbf{r}) \tag{43a}$$

$$\beta_2^2 - 3\mu_t^2(1-a) + i\frac{3\mu_t\omega}{v} = 0. \tag{43b}$$

To solve Eq. (43b), it may be expressed on the form $\beta_2 = \sqrt{x - iy}$. Then β_2 will become

$$\beta_2 = \left\{\sqrt{x^2+y^2}\exp\left(i\arctan(-y/x)\right)\right\}^{\frac{1}{2}} = \tag{44a}$$

$$= \sqrt[4]{x^2+y^2}\left\{\cos\left(\tfrac{1}{2}\arctan(y/x)\right) - i\sin\left(\tfrac{1}{2}\arctan(y/x)\right)\right\}, \tag{44b}$$

where

$$x = 3\mu_t^2(1-a) \tag{45a}$$

$$y = \frac{3\mu_t\omega}{v}. \tag{45b}$$

Combining Eq. (43), (44) and (45) the unknown constants can be determined

$$\alpha_2 = \frac{3\mu_t SA}{4\pi v} \tag{46a}$$

$$\beta_2 = \left\{\frac{(v\mu_t)^2(1-a)^2+\omega^2}{(v/3\mu_t)^2}\right\}^{\frac{1}{4}} \cdot \tag{46b}$$

$$\cdot\left(\cos\left\{\tfrac{1}{2}\arctan\left(\frac{\omega}{v\mu_t(1-a)}\right)\right\} - i\sin\left\{\tfrac{1}{2}\arctan\left(\frac{\omega}{v\mu_t(1-a)}\right)\right\}\right)$$

Eq. (46) and (37) yield an expression for $\rho_2(\mathbf{r})$, which is inserted into Eq. (31a) together with Eq. (42) in order to get an analytical expression for the angular density:

$$\rho(\mathbf{r},t) = \frac{3\mu_t S}{4\pi v r}\exp\left(-r\mu_t\sqrt{3(1-a)}\right) + \tag{47}$$

$$+\frac{3\mu_t SA}{4\pi v r}\exp\left(-r\left\{\frac{v^2\mu_t^2(1-a)^2+\omega^2}{(v/3\mu_t)^2}\right\}^{\frac{1}{4}}\cos\left\{\tfrac{1}{2}\arctan\left(\frac{\omega}{v\mu_t(1-a)}\right)\right\}\right)\cdot$$

$$\cdot\exp\left(ir\left\{\frac{v^2\mu_t^2(1-a)^2+\omega^2}{(v/3\mu_t)^2}\right\}^{\frac{1}{4}}\sin\left\{\tfrac{1}{2}\arctan\left(\frac{\omega}{v\mu_t(1-a)}\right)\right\} - i(\omega t+\varepsilon)\right)$$

For a non-absorbing medium, $a = 1$ and Eq. (47) reduces to

$$\rho(\mathbf{r},t) = \frac{3\mu_t S}{4\pi v r} + \frac{3\mu_t SA}{4\pi v r}\exp\left(-r\sqrt{\frac{3\omega\mu_t}{2v}}\right)\exp\left(ir\sqrt{\frac{3\omega\mu_t}{2v}} - i(\omega t+\varepsilon)\right) \tag{48}$$

Here the first exponential represents the attenuation of the photon density, while the second represents its phase at a distance r. Eq. (47) and (48) reveal two important properties of the propagation of intensity-modulated light by diffusion. First, the intensity-modulated light remains coherent, that is the photon density wave travels with a constant phase velocity. Secondly, the attenuation increases with increasing modulation frequency. From Eq. (48) it is obvious that, in a non-absorbing medium, the photon-density wave from a sinusoidally modulated source at frequency ω is

$$\lambda = 2\pi\sqrt{\frac{2v}{3\mu_t\omega}} \tag{49}$$

and the constant speed of the wave-front is

$$V = \sqrt{\frac{2v\omega}{3\mu_t}} \tag{50}$$

Note that the wavelength in Eq. (49) is the wavelength of the intensity-modulated photon density, not the colour of the light. To get an idea of the size of λ and V, assume that the source is modulated with $\omega \approx 10^9$ rad/s. In tissue light travels with the speed $v \approx 10^{11}$ mm/s and the inverse mean free path $\mu_t \approx 1$ mm^{-1}. If these values are inserted, the wavelength of the photon density wave, given by Eq. (49), is on the order of 50 mm and the speed of the wave-front given by Eq. (50) is on the order of 10^{10} mm/s. It is worth noting the wavelength becomes smaller with a larger μ_t, that is a shorter mean free path. This means that the resolving power of the photon-density waves increases with increased scattering. Eq. (49) also gives that higher modulation frequency of the light source will give an improved resolving power. Unfortunately, an increase in μ_t or ω also leads to a decrease in the amplitude of the modulated signal. Presence of absorption, $a < 1$, will increase the wavelength of the photon density and thus decrease the spatial resolution. When photon transport in a highly scattering media is treated as a diffusional process, the propagation of intensity-modulated light might be considered as a wave-phenomenon. The photon density then constitutes of a scalar field that is propagating at constant speed in a spherical wave. The intensity of the wave at any given point from a number of point sources or localised absorbers can be calculated by superposition.

There is a practical difference in describing the diffusion of photons in the frequency-domain with respect to its Fourier transform equivalent in the time-domain; intensity modulated waves at any frequency propagate coherently, while pulses do not. This is schematically described in Fig. 7. As can be seen in Fig. 7a, a narrow pulse traversing a scattering medium is broadened due to the distribution of optical paths of the photons arriving at the detector. If the medium is thick and strongly scattering, there are no coherent components in the transmitted pulse. If the light source is sinusoidally modulated, on the other hand, the transmitted wave will remain modulated with the same frequency as the incident wave, as shown in Fig. 7b. The reduced amplitude of the transmitted wave is a result of attenuation related to scattering and absorption in the medium.

In Fig. 7b the quantities measured with a frequency domain instrument are shown. These are the phase lag ϕ of the intensity modulated wave relative to the source intensity, the average intensity of the detected signal, that is the DC intensity, and the frequency dependent part of the detected intensity, which is the AC amplitude. These quantities can also be found the solution to the linear transport equation with a sinusoidally modulated

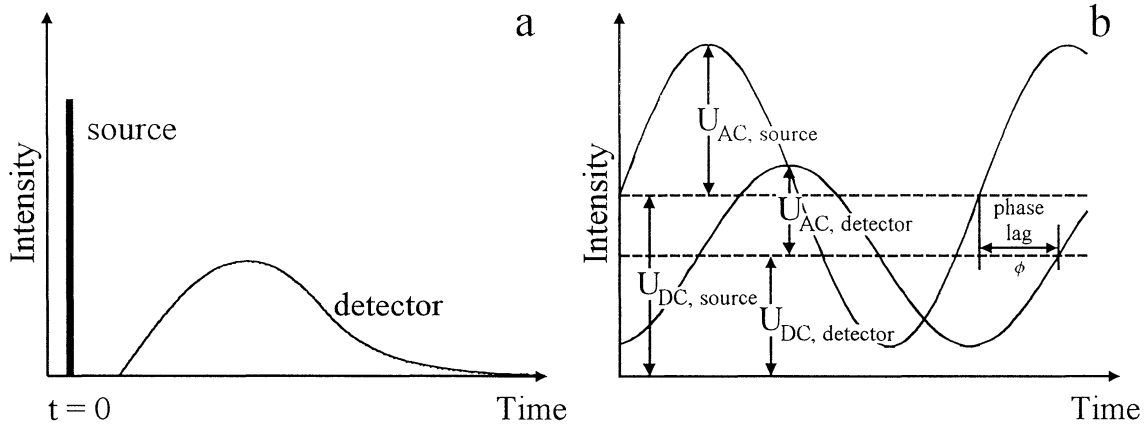

Fig. 7. (a) *Schematic representation of the time evolution of the light intensity measured in response to a very narrow pulse traversing an arbitrary distance in a scattering and absorbing medium.* (b) *The time evolution of the intensity measured when a wave coming from a sinusoidally intensity modulated source traverses the same medium.*

point source, expressed in Eq. (47). However, the measured quantity is not the photon density $\rho(\mathbf{r},t)$, but rather the photon intensity $I(\mathbf{r},t)$, which is given by

$$I(\mathbf{r},t) = v\rho(\mathbf{r},t) \tag{51}$$

From Eq. (47) and (51) the following expression for the phase, the DC intensity and the AC part can be derived:

$$\phi = r\left\{\frac{v^2\mu_t{}^2(1-a)^2+\omega^2}{(v/3\mu_t)^2}\right\}^{\frac{1}{4}} \sin\left\{\tfrac{1}{2}\arctan\left(\frac{\omega}{v\mu_t(1-a)}\right)\right\} - \varepsilon \tag{52}$$

$$\ln(rU_{DC}) = -r\mu_t\sqrt{3(1-a)} + \ln\left(\frac{3\mu_t S}{4\pi}\right) \tag{53}$$

$$\ln(rU_{AC}) = -r\left\{\frac{v^2\mu_t{}^2(1-a)^2+\omega^2}{(v/3\mu_t)^2}\right\}^{\frac{1}{4}} \cos\left\{\tfrac{1}{2}\arctan\left(\frac{\omega}{v\mu_t(1-a)}\right)\right\} + \ln\left(\frac{3\mu_t SA}{4\pi}\right) \tag{54}$$

Worth noting is that all these three expressions are linear functions of the distance between the source and the detector, r, but have a more complicated dependence on the modulation frequency ω, the inverse mean free path μ_t and the albedo a. The linear dependence of ϕ, $\ln(rU_{DC})$ and $\ln(rU_{AC})$ on r is a necessary, but not sufficient, condition for

the validity of the diffusion approximation to the linear transport equation with a sinusoidally intensity modulated point source for the case of photon transport through a very turbid medium.

Further, Fishkin *et al.* have performed measurements that showed good agreement with the theoretical results [18].

4 METHODS AND MATERIALS

4.1 EXPERIMENTAL ARRANGEMENT

In Fig. 8 the experimental arrangement for phase-resolved transillumination is shown. As a light source a Mitsubishi ML 4102-01 laser diode is used. The laser diode emits near-infrared light (3 mW) with a wavelength of 780 nm.

There are three main reasons for using a diode laser in this kind of experiments. Firstly, it is working in the red or near infrared region, where tissue is most transparent. Secondly, it is small, easy to handle and rather inexpensive. Thirdly, it is very easy to modulate with a radio frequency. All that is needed is a signal generator. In this study a Radio Company 1362 UHF Oscillator was used. The signal from the oscillator was divided into two halves with a power splitter. Half of the signal was used as a reference signal at the mixer, see below. The second part was fed together with a DC signal to the laser diode.

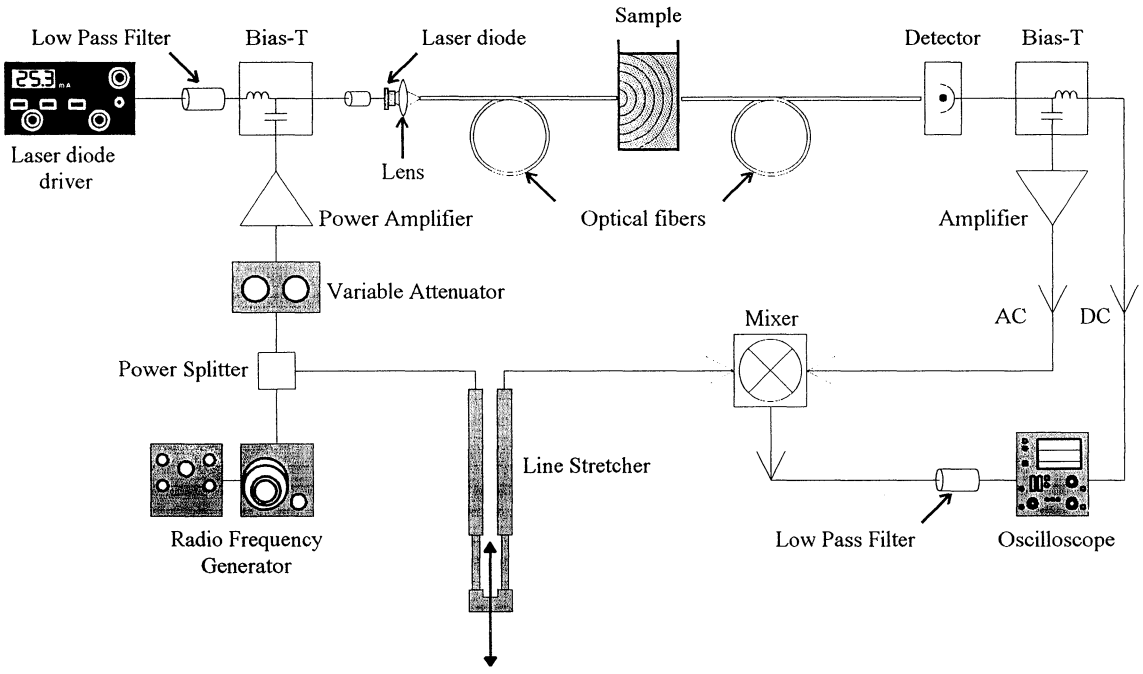

Fig. 8. *The experimental arrangement.*

The modulated laser light was then focused onto an optical fibre. The fibre was made of quartz with a core diameter of 600 μm and had a plastic cladding. The light was transmitted via the fibre to the sample that was to be studied.

4.2 THE DETECTOR

On the detector side the light was collected with another fibre. The length of the fibre was less than one meter and the light was transmitted to a detector.

In this study two different types of detectors has been tested. First a PIN diode, Hamamatsu S4753, was used. However, it turned out that the amount of scattered light collected by the detection fibre was far too little to be measured by the photo diode. Then a photo multiplicator tube, Hamamatsu R928, was tested. Now the detector recorded the scattered light, but the surrounding electronics also picked up some radio frequency signals from the power amplifier. These signals interfered with the interesting ones.

A box made of copper was connected to ground and placed over the power amplifier and the laser diode. Unfortunately, this did not screen the radio frequency as assumed. By moving the sample and the detector to another room, the interfering signals disappeared and it was possible to perform measurements.

4.3 THE MIXER

A mixer is an electronic device that multiplies two signals. Assume that the two signals U_1 and U_2 are on the form:

$$U_1 = A\sin(\omega_1 t + \varepsilon_1) \text{ and } U_2 = B\sin(\omega_2 t + \varepsilon_2). \tag{55}$$

If these signals are multiplied in an ideal mixer, the result will be

$$U = U_1 U_2 = A\sin(\omega_1 t + \varepsilon_1) B\sin(\omega_2 t + \varepsilon_2) \tag{56}$$

Using some trigonometric theorems, this could also be written as

$$U = AB\left\{\cos\left((\omega_1 + \omega_2)t + \varepsilon_1 + \varepsilon_2\right) - \cos\left((\omega_1 - \omega_2)t + \varepsilon_1 - \varepsilon_2\right)\right\} \tag{57}$$

Since both signals originate from the radio frequency oscillator, they both have the same frequency, $\omega_1 = \omega_2 = \omega$. The absolute values of the two phases are not of interest, only the relationship between them. Therefore, it is possible to set them to $\varepsilon_1 = \varepsilon$ and $\varepsilon_2 = 0$. These values are then inserted into Eq. (57), which then will give

$$U = AB\left\{\cos(2\omega t + \varepsilon) - \cos(\varepsilon)\right\} \tag{58}$$

If this signal is low pass-filtered, the remaining signal is a DC-level, which is only dependent on the cosine of the phase difference between the two mixed signals. The difference in phase is proportional to the difference in path length. The phase of the

detected signal alters as the scattering coefficient varies, while the phase of the reference signal can be changed by the line stretcher.

When a laser diode is modulated sinusoidally, the output is not a pure sinus function, but has harmonics. These will cause harmonics from the mixer too, but since the signal is low pass-filtered, there will be no contributions from them in the examined signal.

4.4 THE SAMPLE

The sample is supposed to simulate tissue. Therefore it needs to have good scattering characteristics. Using a scattering liquid in a cuvette as a tissue phantom makes it easy to alter the optical properties of the phantom. Absorption can be accomplished by adding ink to the liquid. It is also easy to place a phantom tumour within the sample. By placing the cuvette in a movable holder, scanning can easily be performed. These features have not been employed during this study.

In this study the sample consisted of a glass cuvette containing a scattering liquid. The inner dimensions of the cuvette were 95 mm wide, 95 mm high and 30 mm deep. Thus the light has to travel at least 30 mm through the sample. The scattering liquid used is a liquid called Intralipid 200 mg/ml (Kabi Vitrum, Stockholm). This liquid is a fat emulsion used clinically as an intravenously administered nutrient. The liquid is white and looks much like milk. The scattering particles consist of soybean oil encapsulated within a monolayer of lecithin [26].

5 RESULTS

As previously mentioned, it was impossible to do any measurements when all the equipment was placed in the same room. The modulation signal was transmitted into the room and picked up in the detector electronics. Therefore, the light from the laser was conducted to another laboratory with a long fibre. In this laboratory the sample, the detector, the line stretcher and the mixer were placed. Thanks to the great distance between the source and the detector, the problem with the radio frequency interference was eliminated.

In Fig. 9, the AC component of the detected signal is shown. The two curves are measured when the cuvette was filled with pure water and with Intralipid added, respectively. The signals are the average over 1000 scans of a digital oscilloscope. As can be seen, the phase lag due to increased scattering properties is easily detectable, even when the scattering coefficient is relatively low.

The first real measurements were made to see how the equipment responded to a varying scattering coefficient. The cuvette was filled with 200 ml water. With the line stretcher, the two signals were phase matched, which could be seen as a maximum signal from the mixer. The Intralipid was diluted with a factor 20, i.e. the solution contained 10 mg/ml. From this solution 0.5 ml was added to the cuvette between each measuring point. After

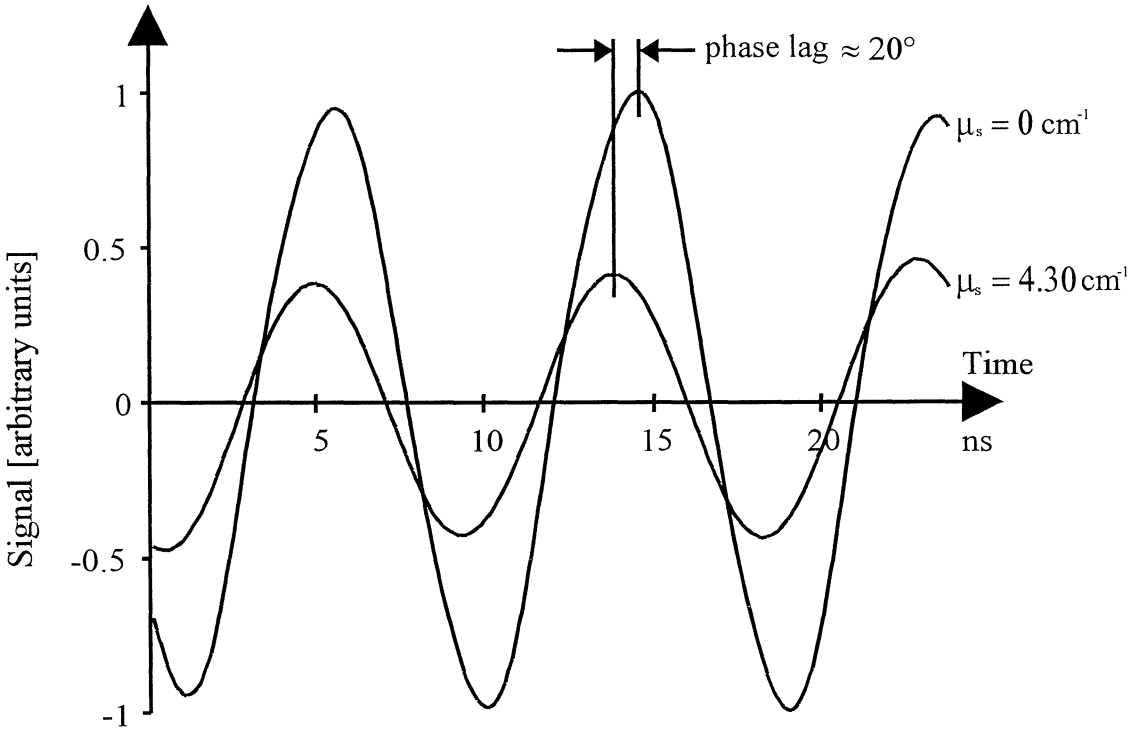

Fig. 9. *The phase lag due to increased scattering properties of the sample. The curves are the averages of 1000 measurements of the AC component of the signal from pure water and an Intralipid solution, respectively.*

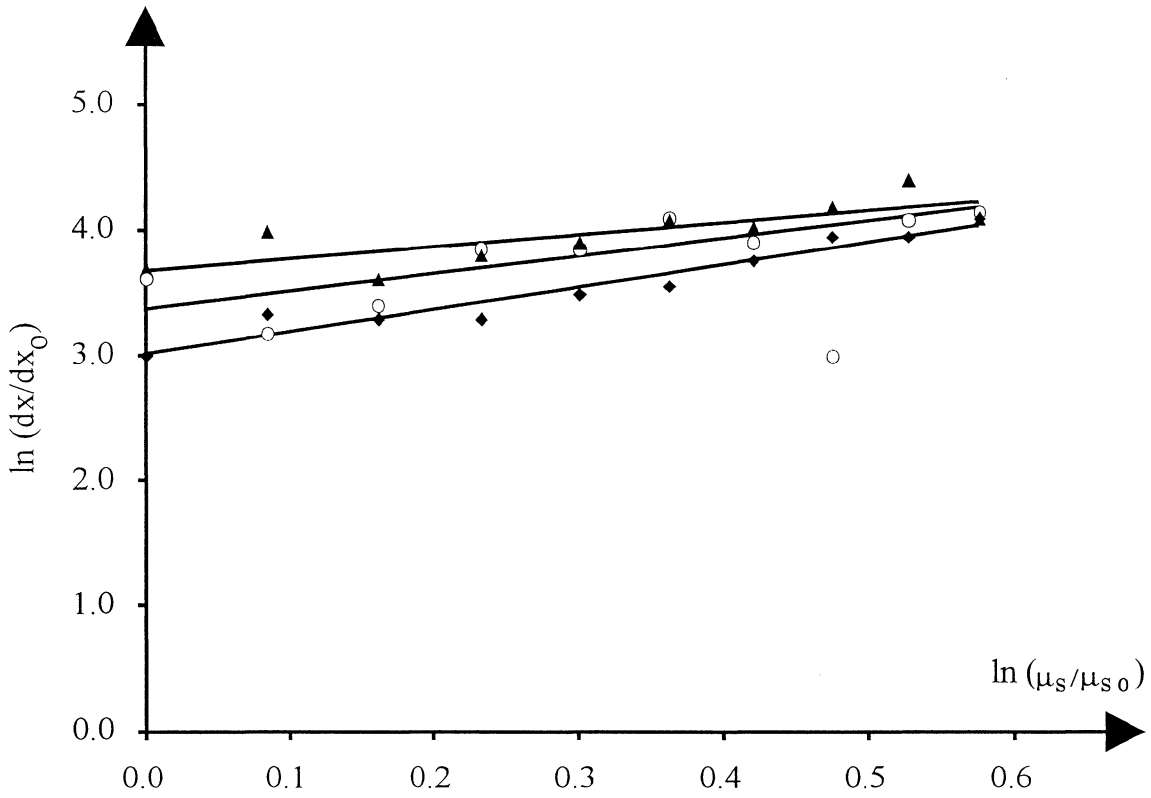

Fig. 10. *The relative position of the line stretcher, when the reference signal and the detected signal were in phase, as a function of the scattering coefficient (logarithmic plot). Repetitive measurements.*

each addition of Intralipid, four variables were measured; the DC level from the amplifier, the signal from the mixer with the line stretcher in the position where the two signals were in phase for pure water, the maximum of the mixed signal and the corresponding position of the line stretcher. In Fig. 10, the logarithm of the difference in path length of the reference signal is plotted as a function of the logarithm of the scattering coefficient. There were some difficulties measuring the mixed signal. The amplitude of the detected signal was not constant in time, but varied irregularly. This made the mixed signal vary too. As a result, it was hard to determine the exact position of the line stretcher, where the two signals were in phase. From the few measurements made, it is impossible to determine the phase lag as a function of the scattering coefficient, but it seems as there is a linear relationship in the logarithmic plot. This seems to correspond to the theory. Further measurements are required.

In Fig. 11, the DC level of the detected signal is plotted versus the scattering coefficient. Due to saturation at the detector when the scattering coefficient was low, the expontential fit is not valid there.

As mentioned above, too few measurements have been performed and the results have had a too large variation to make it possible to make any quantitative statements. However,

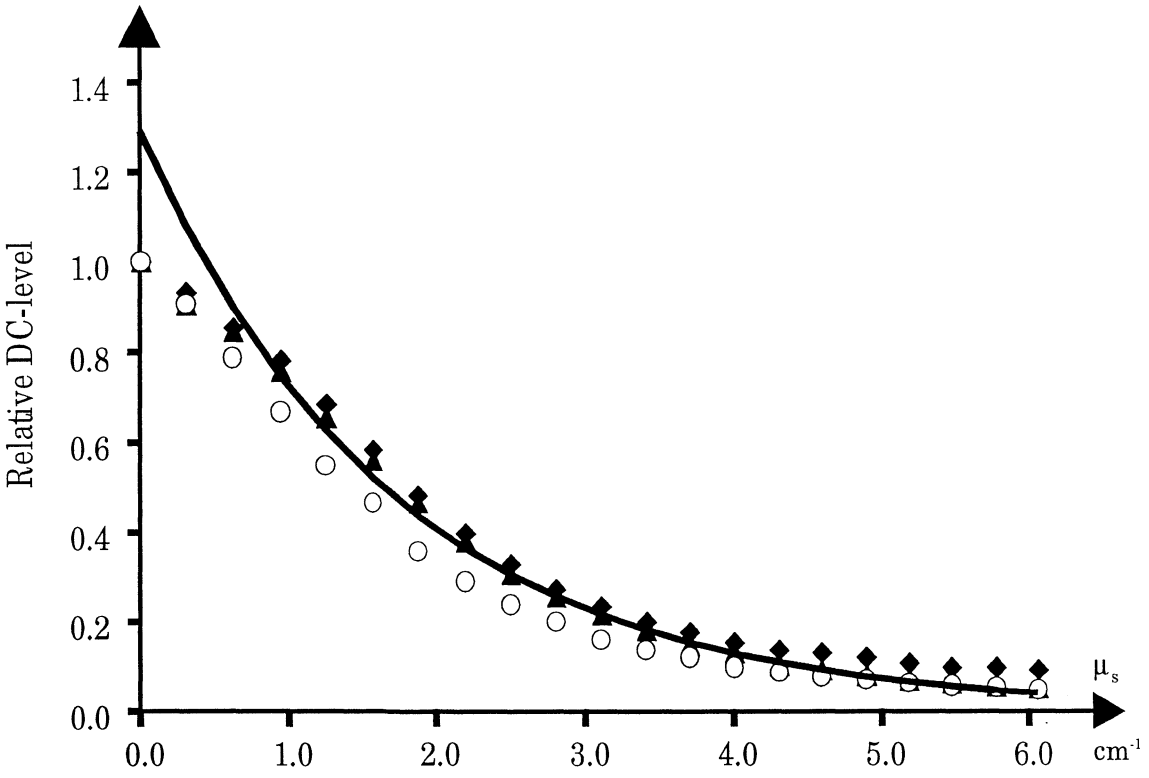

Fig 11. *The DC level of the detected signal plotted versus the scattering coefficient.*

these preliminary results suggest that the technique might be useful, in spite of the relatively simple and inexpensive equipment used.

6 Discussion and Conclusions

6.1 Problems

The greatest problem during this study has been to get rid of the interfering radio-frequency signals. Using the same frequency for both modulation and detection seems to be very difficult. A lot of work has been done to localise the source and try to shield that and the detector.

When trying to shield the radio-frequency it is important to remember that it is the longest extension of an opening in the metal that determines whether there will be a leak or not. To let any radio-frequency out there must be a slit that is at least of the same length as the wavelength of the radio-frequency. The area of a hole is not important.

To look at the radio-frequency in the room the detector was turned off. The signal amplifier was still working. If the amplifier was connected to the detector and the oscillator was working, the radio-frequency could be seen on an oscilloscope. While looking at the signal from the amplifier, not connected to the detector, only the noise from the amplifier could be seen. Thus, it was in the detector, especially when working with a photomultiplier, that the interfering signals were collected.

The photomultiplier housing was originally built for three photomultipliers. Due to that there where three coaxial cables going out of which only one was used. The two other cables worked as antennas. They were covered with aluminium foil, which reduced the signal. To alter the high voltage to the detectors a potentiometer outside the housing was connected to the high voltage generator within the housing. This cable also worked as an antenna and therefore the potentiometer was placed within the case instead.

To get rid of the radio-frequency pick-up in the electronics, the sample and the detector had to be moved to another room. In this way, it was possible to perform some measurement, but it is not practically satisfactory.

6.2 The Future

To minimise the radio-frequency pick-up on the detector side a new housing is being considered. It is planned that it shall contain the same photomultiplier as before, Hamamatsu R928. The socket is to be replaced with a socket that contains a high voltage generator. The socket is then biased with a DC that can be varied from 0V to 15V. This is easily accomplished with a 15V voltage source and a potentiometer. The voltage source can also be used to bias the signal amplifier, which also is going to be placed within the new box. This is done mainly to reduce the length of the cable between the detector and the amplifier to reduce the amount of noise being amplified. With this arrangement a minimum number of cables connecting this box to the rest of the equipment is needed. The essential inputs are a hole for an optical fibre and a 220V AC cable. From the box there

will only be one output, a coaxial cable with the amplified signal. On the outside there will also be an on/off switch and a knob for the potentiometer that controls the high voltage.

Hopefully, this will reduce most of the pick-up on the detector side. To reduce the interference further, a similar box for the light source is also being considered. The main source seems to be either the power amplifier, the bias-tee (where the signal from the laser diode driver and the oscillator are superimposed) or the connection between the cables and the partially free connection pins of the laser diode. The cable that connects the variable attenuator with the power amplifier also seems to influence the emission. That the oscillator does not leak any radio-frequency is shown by just turning it on and turn the variable attenuator to maximum attenuation. Then there is no signal on the detector side. A box that contains the laser, the bias-tee and the power amplifier with its bias supply could perhaps decrease the radiation of radio-frequency in the laboratory.

If all these efforts to minimise the radio-frequency in the room are not successful the cross-correlation technique described in chapter 2.8.2 will be considered. Since the light source and the detector are modulated with two slightly different radio-frequencies and all measurements are made on the cross-correlation signal, there will be no interference from the modulation signal as long as the light modulation signal is not picked up in the photomultiplier dynodes. The experimental arrangement is more complicated and will require more and expensive equipment.

To use type of phase-resolved measurements described in this paper clinically, some kind of scanning equipment must be developed. Even better would it be if a whole image could be made in one measurement. A possible approach could be to use a CCD array detector in conjunction with a modulated image intensifier (see e.g. [18]).

6.3 CONCLUSIONS

Theoretically, the idea of using phase-resolved measurements to detect objects with different optical properties inside a turbid medium, such as tissue, is promising. Preliminary results from measurements with the equipment described in this study and some practical results with the cross correlation technique also point in that direction.

7 ACKNOWLEDGMENTS

I would like to thank everyone who has helped me to complete this study. Some of them are worth to be mentioned by name.

First of all I would like to thank Roger Berg and Stefan Andersson-Engels, who have guided me through my work.

Without the help with laser diodes, amplifiers and mixers from Peter Kauranen, this work would have been impossible to perform. He has also given me some pieces of advice concerning the difficulties in working in the radio frequency region.

I would also like to thank Åke Bergquist, who has been very helpful when new electronic equipment has been constructed or old things have needed to be repaired.

When I have been struggling with my equipment and not been able to see an end to the problems, it has been very good to have Ulf Gustafsson to talk with. I wish him good luck with his equipment and the work with his diploma paper.

Finally, I would like to thank professor Sune Svanberg. It is thanks to his lectures and enthusiasm that I have become interested in this field of physics. He has also been very helpful to make me get some experimental results from this study.

This work was supported by the Swedish Research Council for Engineering Sciences, the National Board for Industrial and Technical Development, the Swedish Cancer Society and by the Department of Diagnostic Radiology, Lund University Hospital.

8 LIST OF REFERENCES

1. J. Ewing, "Neoplastic disease", Edited by W.B. Saunders, Philadelphia, 1928.

2. M. Cutler, "Transillumination as an Aid to Diagnosis of Breast Lesions", Surg., Gynecol. and Obstet. **48**:721-727, 1929.

3. O. Jarlman, "Diagnostic Transillumination of the Breast", Dissertation Thesis, University Hospital, Lund, 1991.

4. H. Noltenius, "*Human Oncology*", Urban & Schwarzenberg, Baltimore - Munich, 1981.

5. R. Bernro, and I. Pettersson, "Electromagnetic Waves in Tissue", Diploma Paper, Lund Institute of Technology, 1987.

6. R. Berg, "Time-Resolved Studies of Light Propagation in Tissue", Diploma Paper, Lund Institute of Technology, Lund Reports on Atomic Physics **LRAP-106**, 1989.

7. M. Swift, D. Morrell, R.B. Massey, and C.L. Chase, "Incidence of Cancer in 161 Families Affected by Ataxia-Telangiectasia", N. Engl. J. Med. **325**:1831-1836, 1991.

8. H.J. Isard, "Other Imaging Techniques", Cancer **53**:658-664, 1984.

9. C.M. Gros, Y. Quenneville and Y. Hummel, "Diaphanologic mammaire", J. Radiol. Electrol. Med. Nucl. **53**:297, 1972.

10. B. Ohlsson, J. Gundersen and D.-M. Nilsson, "Diaphanography: A Method For Evaluation of the Female Breast", World J. Surg. **4**:701-707, 1980.

11. E.N. Carlsen, "Transmission Spectroscopy: An Improvement in Light Scanning", RNM Images, February 1983.

12. R. Berg, O. Jarlman and S. Svanberg, "Medical Transillumination Imaging Using Short-Pulse Diode Lasers", Appl. Opt. **32**:574- 579, 1993.

13. S. Andersson-Engels, R. Berg and S. Svanberg, "Effects of Optical Constants on Time-Gated Transillumination of Tissue and Tissue-Like Media", J. Photochem. Photobiol., B: Biol. **16**:155-167, 1992.

14. S. Andersson-Engels, R. Berg, S. Svanberg and O. Jarlman, "Time-Resolved Transillumination for Medical Diagnostics", Opt. Lett. **15**:1179-1181, 1990.

15. J.R. Lakowicz, G. Laczko, I. Gryczynski, H. Szmacinski, W. Wiczk and M.L. Johnson, "Frequency-Domain Fluorescence Spectroscopy; Principles, Biochemical Applications and Future Developments", Ber. Bunsenges. Phys. Chem. **93**:316-327, 1989.

16. B.A. Feddersen, D.W. Piston and E. Gratton, "Digital Parallel Acquisition in Frequency Domain Fluorimetry", Rev. Sci. Instrum. **60**:2929-2936, 1989.

17. J. Fishkin, E. Gratton, M.J. vandeVen and W.W. Mantulin, "Diffusion of Intensity Modulated Near-Infrared Light in Turbid Media", Proc. SPIE Time-Resolved Spectroscopy and Imaging of Tissues, **SPIE 1431**:122-135, 1991.

18. K.W.Berndt and J.R. Lakowicz, "Detection and Localization of Absorbers in Scattering Media Using Frequency Domain Principles", Proc. SPIE Time-Resolved Spectroscopy and Imaging of Tissues, **SPIE 1431**:149-160, 1991.

19. E. Gratton, W.W. Mantulin, M.J. vandeVen, J.B. Fishkin, M.B. Maris and B. Chance, "Imaging of Tissues Using Intensity-Modulated Near-Infrared Light", Science, (to appear).

20. S. Ertefai and E. Profio, "Spectral Transmittance and Contrast in Breast Diaphanography", Med. Phys. **12**:393-400, 1985.

21. J.-L. Boulnois, "Photophysical processes in laser-tissue interactions", In: R. Ginsberg (ed) "*Laser Applications in Cardiovascular Diseases*", Futura, New York, 1987.

22. P. Parsa, S.L. Jacques and N.S. Nishioka, "Optical Properties of Rat Liver Between 350 and 2200 nm", Appl. Opt. **28**:2325-30, 1989.

23. A. Ishimaru, "*Wave Propagation and Scattering in Random Media*", Academic Press, New York, 1978.

24. S. Andersson-Engels, "Laser-Induced Fluorescence for Medical Diagnostics", Dissertation Thesis, Lund Institute of Technology, Lund Reports on Atomic Physics **LRAP-108**, 1989.

25. K.M. Case and P.F. Zweifel, "*Linear Transport Theory*", Addison-Wesley Publishing Co., Inc., Reading, MA, Palo Alto, London, Don Mills, Ontario, 1967.

26. L. Stryer, "*Biochemistry*", Freeman, San Francisco, California, 1981.